Proton gap due to the necking potential

R. A. Gherghescu,[1,*] D. N. Poenaru,[1] and W. Greiner[2]
[1]*Horia Hulubei-National Institute for Nuclear Physics and Engineering, P. O. Box MG-6, RO-76900, Bucharest, Romania*
[2]*Frankfurt Institute for Advanced Studies, Ruth-Moufang Str. 1, D-60438 Frankfurt am Main, Germany*
(Received 5 October 2007; revised manuscript received 29 June 2008; published 25 August 2008)

A smooth necking region between fission fragments is obtained by rolling a sphere around the symmetry axis of the nuclear shape formed by two intersected spheroids. The potential generated by the necking nucleons is obtained from potential theory, imposing the condition of equipotentiality on the nuclear surface. The final result is a two-Nilsson type potential linked by the necking potential. The proton and neutron level scheme is calculated for ^{236}Pu along the ^{92}Se + ^{144}Nd fission channel, and a gap is obtained for a certain neck geometry, leading to a negative proton shell correction energy able to accommodate a shape isomer.

DOI: 10.1103/PhysRevC.78.024604 PACS number(s): 25.70.Jj, 21.60.Ev, 21.60.Cs

I. INTRODUCTION

The influence of deformation parameters upon the fission process is always taken into account to lower the height of the barrier. One of these parameters appears as a smooth necking region that develops between the nascent fragments when fission takes place [1,2]. Necked fission configuration parametrized with Cassini ovaloids [3] or in a dumbbell shape [4], though describing correctly the neck, do not reach separated daughter and emitted fragment level schemes. A simulation of the two-center nuclear shape with a neck is made in Ref. [5] and a first attempt to introduce the neck microscopically by means of a smoothing function appears in Ref. [6]. The goal of the present work is to use a microscopic neck potential based on potential theory as part of the deformed two-center shell model. A particular result appears for the numerical application on the fission channel ^{92}Se + ^{144}Nd from ^{236}Pu, where an energy gap is emphasized within a certain necked fission configuration.

II. NECK POTENTIAL

The calculations are based on the deformed two-center shell model presented in Ref. [7]. The binary shape describing a fission configuration with a neck region between the spheroidal fragments is displayed in Fig. 1. The geometrical quantities that are used further on are explained: z_H and z_L are the centers of the heavy (H) and light (L) spheroid, R_3 is the radius of the sphere tangent to the fragments and shaping the neck region, (z_3, ρ_3) are the coordinates of the necking sphere center, and R is the distance between the two centers. The initial configuration corresponds to the parent nucleus shape with semiaxes (a_0, b_0). At the beginning the emitting fragment is entirely enclosed in the parent and tangent to its inner surface. Therefore the starting point of the process coincides with the configuration where the distance between centers is $R_i = a_0 - a_L$. At the end of the process, the distance between centers equals $R_f = a_H + a_L + 2R_3$, the two spheroids are completely separated, and the neck sphere is aligned with the fragments. The Nilsson potentials generating the mean field of nucleons confined within two spheroids are described by

$$\begin{aligned} V_H(\rho, z) &= \tfrac{1}{2}m_0\omega_{\rho_H}^2\rho^2 + \tfrac{1}{2}m_0\omega_{z_H}^2(z + z_H)^2 \\ V_L(\rho, z) &= \tfrac{1}{2}m_0\omega_{\rho_L}^2\rho^2 + \tfrac{1}{2}m_0\omega_{z_L}^2(z - z_L)^2, \end{aligned} \tag{1}$$

where H and L stand for heavy and light, ω_{ρ_H} and ω_{ρ_L} are the frequencies on the $O\rho$ axis, and ω_{z_H} and ω_{z_L} are the corresponding frequencies on the symmetry axis. The value z_H and z_L are the centers of the heavy and light fragments, respectively, on the Oz axis.

As one rolls an outside sphere around the symmetry axis, by keeping it tangent to the two spheroidal intersected fragments, the necking region is generated as a spherical curve from one tangent point to the other. If the force is considered central in the necking region,

$$\vec{F}(\vec{r}) = -C\vec{r}, \tag{2}$$

one obtains, by integrating up to the nuclear surface $\vec{r}(\rho, z)$,

$$V_{g1}(r) = V_c - \frac{Cr^2}{2}, \tag{3}$$

where the constant V_c is determined from the equipotentiality condition. If one considers an oscillator type force, it is reasonable to have $C = m_0\omega_g^2$; hence, the force in the necking region will be

$$\vec{F}(\vec{r}) = -m_0\omega_g^2\vec{r}. \tag{4}$$

To recover the tangent sphere, one replaces $r(\rho, z)$ by the corresponding spherical neck generating function $r^2 = (\rho - \rho_3)^2 + (z - z_3)^2$, where (ρ_3, z_3) is the center of the sphere. It results the outer neck potential as

$$V_{g1}(r) = 2V_0 - \frac{m_0\omega_g^2}{2}[(\rho - \rho_3)^2 + (z - z_3)^2], \tag{5}$$

where V_0 is the constant value on the nuclear surface. There is also the inside region of the nuclear shape, between the two spheroid surfaces and the neck, where the potential is constant $V_{g2}(\rho, z) = V_0$ (no potential gradient). The value of V_0 is obtained from two well-known relations: $\hbar\omega = 41\ \mathrm{A}^{-1/3}$, which

*rgherg@ifin.nipne.ro

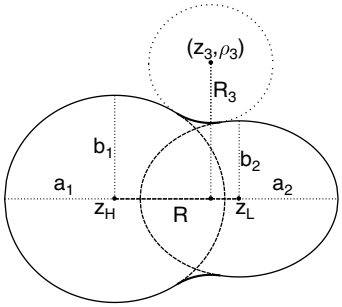

FIG. 1. Fission configuration and deformation coordinates within the necked two-center shell model.

relates the assigned frequency to the corresponding nuclear mass A, and $R = r_0\, A^{1/3}$, where R is the radius of the nucleus of mass A. By multiplying the first relation with m_0c^2 (the nucleon mass in MeV) and accounting for $m_0\omega^2R^2/2 = V_0$ (the potential value at the surface of the nucleus with radius R) we obtain, for r_0=1.16, the value $V_0 = 27.14$ MeV. One must observe that the A dependence is canceled, so the value of V_0 is the same for all nuclei. Within the same reasoning, the neck frequency ω_g is obtained from the value of the neck potential at a radius $R = R_3$ (the distance from the sphere center down to the surface of the neck region), namely, $m_0\omega_g^2R_3^2 = V_0$, which numerically relates the neck potential to the geometry of the neck. The complete expression of the microscopic potential complies with the condition of equipotentiality on the nuclear surface.

Finally one obtains the potential that generates a binary fission necked type shape:

$$V_{\rm osc}(\rho,z) = \begin{cases} V_H(\rho,z), & v_H \\ V_g(\rho,z) \\ V_L(\rho,z), & v_L, \end{cases} = \begin{cases} V_{g1}(\rho,z), & v_{g1} \\ V_{g2}(\rho,z), & v_{g2} \end{cases} \tag{6}$$

where v_H and v_L are the space regions where the potentials $V_H(\rho,z)$ and $V_L(\rho,z)$ are active and, similarly, v_{g1} and v_{g2} are the regions where the two neck-related potentials V_{g1} and V_{g2} intervene in the calculations of the corresponding matrix elements to obtain the single particle energies. These regions are also visualized in Ref. [7].

To obtain the total Hamiltonian, one must add the spin-orbit and the $\mathbf{\Omega}^2$ term, where $\mathbf{\Omega}$ is the deformation-dependent angular momentum operator:

$$\left[-\frac{\hbar^2}{2m_0}\Delta + V_{\rm osc}(\rho,z) + V_{\mathbf{\Omega s}} + V_{\mathbf{\Omega}}^2\right]\Psi = E\Psi. \tag{7}$$

The Schroedinger equation for this binary potential is solved following the procedure described in Ref. [7]. The form of the angular momentum operator for the neck region is adapted to the binary configuration. One uses the anticommutator to ensure the hermicity of the spin-orbit operator:

$$V_{\mathbf{\Omega s}} = -\left\{\frac{\hbar}{m_0\omega_{0i}}\kappa_i(\rho,z), (\nabla V_{\rm osc}\times\mathbf{p})\,\mathbf{s}\right\}, \quad A_i - \text{region}, \tag{8}$$

where $i = H$ (heavy) or L (light), and the strength of the interaction $\kappa_i(\rho,z)$ varies with the nuclear mass region. The potential $V_{\rm osc}$ is replaced successively with V_H, V_{g1}, and V_L in the previous formula. One uses for the spin-orbit operator the usual expression:

$$\mathbf{\Omega s} = \tfrac{1}{2}(\mathbf{\Omega}_+\mathbf{s}_- + \mathbf{\Omega}_-\mathbf{s}_+) + \mathbf{\Omega}_z\mathbf{s}_z, \tag{9}$$

where the subscripts $+$ and $-$ hold for the creation and anihilation operators, respectively. As a consequence one obtains for the creation, anihilation, and z terms of the angular momentum operators in the neck region v_{g1}

$$\begin{aligned}
\mathbf{\Omega}^+(v_{g1}) &= -e^{i\varphi}\left[\frac{\partial V_g(\rho,z)}{\partial\rho}\frac{\partial}{\partial z} - \frac{\partial V_g(\rho,z)}{\partial z}\frac{\partial}{\partial\rho}\right.\\
&\quad\left. - \frac{i}{\rho}\frac{\partial V_g(\rho,z)}{\partial z}\frac{\partial}{\partial\varphi}\right]\\
&= -e^{i\varphi}\left[m_0\omega_g^2(\rho-\rho_3)\frac{\partial}{\partial z} - m_0\omega_g^2(z-z_3)\frac{\partial}{\partial\rho}\right.\\
&\quad\left. - \frac{i}{\rho}m_0\omega_g^2(z-z_3)\frac{\partial}{\partial\varphi}\right]\\
\mathbf{\Omega}^-(v_{g1}) &= -e^{i\varphi}\left[\frac{\partial V_g(\rho,z)}{\partial\rho}\frac{\partial}{\partial z} - \frac{\partial V_g(\rho,z)}{\partial z}\frac{\partial}{\partial\rho}\right.\\
&\quad\left. + \frac{i}{\rho}\frac{\partial V_g(\rho,z)}{\partial z}\frac{\partial}{\partial\varphi}\right]\\
&= e^{-i\varphi}\left[m_0\omega_g^2(\rho-\rho_3)\frac{\partial}{\partial z} - m_0\omega_g^2(z-z_3)\frac{\partial}{\partial\rho}\right.\\
&\quad\left. + \frac{i}{\rho}m_0\omega_g^2(z-z_3)\frac{\partial}{\partial\varphi}\right]\\
\mathbf{\Omega}_z(v_{g1}) &= -\frac{i}{\rho}\frac{\partial V_{g1}}{\partial\rho}\frac{\partial}{\partial\varphi} = im_0\omega_g^2\frac{\rho-\rho_3}{\rho}\frac{\partial}{\partial\varphi}.
\end{aligned} \tag{10}$$

The final step in the calculation is the diagonalization of the remaining neck potential $V_{gH,L}$ and spin-orbit operators [Eq. (10)], resulting in the level scheme for protons and neutrons. Then the Strutinsky method [8] yields the proton and neutron shell corrections. Calculations have been performed for a range of the neck-generating sphere radii spanning from $R_3 = 0$ (no neck, fusion-like shapes) to 10 fm, applied to the fission of ^{236}Pu along the fission channel ^{92}Se + ^{144}Nd. This channel has been chosen following the reported mass yield in Ref. [9], where a peak around the heavy mass of $M_H = 141$ corresponding to $\eta_A = (A_h - A_L)/A \approx 0.2$ was obtained.

III. FISSION DYNAMICS

The dynamics of the process involves three main stages: (1) the calculation of the total deformation energy as the sum of the shell corrections and the liquid drop energies, (2) the inertia tensor computation with emphasis on the neck

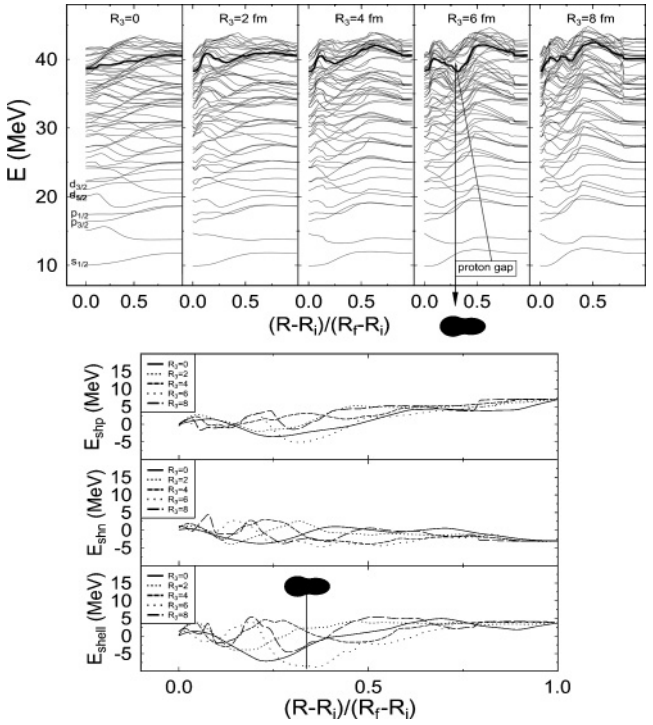

FIG. 2. Five proton level schemes at five different neck radii R_3 (upper plot). Corresponding proton $E_{\rm shp}$, neutron $E_{\rm shn}$, and total $E_{\rm shell}$ shell corrections as functions of the reduced distance between centers (lower plot).

coupling influence, and (3) the construction of the action integral followed by the minimization in the multidimensional space of deformation to obtain the fission path.

A. The shell corrections

The proton $E_{\rm shp}$ and neutron $E_{\rm shn}$ shell corrections are calculated separately due to the difference in the spin-orbit strength interactions. The final results are summed and the total shell corrections are obtained as

$$E_{\rm shell} = E_{\rm shp} + E_{\rm shn}. \tag{11}$$

In the upper part of Fig. 2, five of the calculated proton level schemes are drawn for neck radii $R_3 = 0$, 2, 4, 6, 8 fm, as a function of the reduced distance between centers. R_i and R_f are the initial (emitted fragment totally embedded in the parent nucleus) and final (daughter and emitted nucleus totally separated) distance between centers.

The proton Fermi level is emphasized with a bold line. As a general trend one observes an increase of the energy levels with increasing R_3, especially in the last part of the splitting process. This behavior is due to the fact that the neck potential has values higher than those of the two Nilsson ones for the fragments in the inner neck region. One observes the development of a gap between the Fermi and the first nonoccupied proton level for a neck radius value around $R_3 =$ 6 fm. The gap is located at a reduced distance between centers of $(R - R_i)/(R - R_f) \approx 0.3$ or at a distance between centers of $R = 8.94$ fm. The semiaxis ratios are $\chi_H = b_H/a_H = 0.98$ for the heavy fragment (corresponding to $\beta_2^{(H)} \approx 0.014$) and $\chi_L = b_L/a_L = 0.74$ for the light fragment (corresponding to $\beta_2^{(L)} \approx 0.22$). The total length of the shape is found as $L = 20.13$ fm, which roughly corresponds to a one-nucleus deformation of $\beta_2 = 0.4$ and having the same mass. The total length of the shape at the isomer energy minimum is $L = a_H^{(i)} + a_L^{(i)} + R$, where $a_H^{(i)}$ and $a_L^{(i)}$ are the intermediary semiaxes along Oz and R is the distance between centers at this point ($R = 8.94$ fm). For the semiaxis ratios $\chi_H = 0.98$ and $\chi_L = 0.74$, the volume conservation condition yields $a_H^{(i)} = 6.21$ fm and $a_L^{(i)} = 4.98$ fm. The z coordinate of the center of the necking sphere is between z_H and z_L, and its radius is $R_3 = 6$ fm for this configuration (see Fig. 1). A gap is already observed in other studies. In Ref. [10], self-consistent Hartree–Fock calculations result in the development and reduction of the neutron gap between the Fermi level and the first unoccupied one, at half of the final elongation value. In the macroscopic-microscopic work on ^{240}Pu [1], with another type of binary potential, a proton gap has been found at $\beta_2 \approx 0.3$ for 98 protons. The first work which introduced the neck in a two-center shell model [6] obtained a second minimum in the shell corrections due to a proton gap, but for a much lighter nucleus. The proton gap obtained in the present work exerts its influence upon the shell corrections, presented in the lower part of Fig. 2, where the proton $E_{\rm shp}$, neutron $E_{\rm shn}$, and total shell correction energy $E_{\rm shell} = E_{\rm shp} + E_{\rm shn}$ are plotted. The minimum in $E_{\rm shp}$ for $R_3 \approx 6$ fm will lower the total deformation energy, i.e., the fission barrier. The fission channel will follow the path calculated by minimization of the action integral, which is mostly influenced by the deformation energy value. Though the inertia tensor will also have its importance, minima within the total deformation energy will strongly influence the fission path. Because such a gap is formed, the corresponding configuration becomes (quasi-) stable at this point. The necking potential expressions [Eqs. (5) and (6)] have been obtained using the potential theory with a starting hypothesis of an oscillator type force [Eq. (2)]. This first part of the reasoning ended up with Eq. (4) for the force and consequently with Eq. (5) for the potential. At this stage the only arbitrary assumption is to consider the necking region between the fragments as a concave spherical one, tangent to the two spheroids. But the R_3 value, though treated as a free parameter, increases the multidimensionality of the deformation space (which is one of the main purposes of this work) and induces the exact microscopic potential expressed by Eq. (5). The neck radius R_3 increases the number of degrees of freedom in the fission shape description similar to adding the β_4 parameter to the (β_2, β_3) coordinate space and applying the Woods-Saxon potential for a one-center shell model to simulate the neck. R_3 is fixed arbitrary as a free coordinate, but it generates a new microscopic potential V_g that changes the way the level scheme transits from the parent to two separated fragments. The total deformation energy has been obtained using the macroscopic-microscopic method. The Yukawa-plus-exponential model provided the liquid drop part $E_{\rm LDM}$, and the shell corrections $E_{\rm shell}$ were obtained from the Strutinsky method, as mentioned above. One obtains the

total deformation energy $E_{\rm def}$,

$$E_{\rm def}(q) = E_{\rm LDM}(q) + E_{\rm shell}(q), \tag{12}$$

as a local function of all four deformation parameters q.

B. The inertia tensor and the fission path

This work uses the Werner-Wheeler method to calculate the inertia tensor. It assumes the motion of an irrotational flow and no microscopic effects are included. All possible couplings between the four degrees of freedom (χ_H, χ_L, R_3, R) are taken into account. Because (i) R_3 changes the nuclear shape at every R and (ii) the change of the shape is reflected in the variation of the shell corrections via proton and neutron level schemes, R_3 is part of the collective coordinates and its change affects the way the others degrees of freedom vary. Consequently R_3 generates new couplings with χ_H, χ_L, and R. These couplings express their influence through the inertia tensor components: $B_{R_3R_3}$, $B_{\chi_H R_3}$, $B_{\chi_L R_3}$, B_{RR_3}. The dynamics involves the whole tensor of inertia B, which, when contracted along R, is expressed as

$$\begin{aligned} B(R) = {} & B_{RR} + 2B_{RR_3}\frac{dR_3}{dR} + 2B_{R\chi_H}\frac{d\chi_H}{dR} + 2B_{R\chi_L}\frac{d\chi_L}{dR} \\ & + 2B_{\chi_H\chi_L}\frac{d\chi_H}{dR}\frac{d\chi_L}{dR} + B_{R_3R_3}\left(\frac{dR_3}{dR}\right)^2 \\ & + 2B_{R_3\chi_L}\frac{dR_3}{dR}\frac{d\chi_L}{dR} + 2B_{R_3\chi_H}\frac{dR_3}{dR}\frac{d\chi_H}{dR}, \end{aligned} \tag{13}$$

where the laws of variation (not unique) of other degrees of freedom with R are explained further on in the text.

A fission isomer is possible, like the one revealed in Ref. [11] for ^{236}Pu, where an axis ratio of 2 and a lifetime of about 40 ps are estimated. The gap obtained for $(A_L, A_H) = (92, 144)$ is very close to the experiment [9]. The minimum generated at a certain neck radius is able to sustain a quasistable state for a fission isomer. Evidently, the macroscopic part must be added, but one should account for the fact that its behavior is rather smooth. Consequently, either a short-life shape isomer or a favorable fission path will benefit from the appearance of the energy gap at the Fermi level. Such a gap is the result of the new microscopically introduced neck parameter. The gap is shallower for the neighboring fission channels, but still exists for $(A_L, A_H) = (94, 142)$ and $(90, 146)$. Beyond these values, even when the neck is varied from $R_3 = 0$ to 8 fm, there is no gap at the proton Fermi level. From the experimental results published in Ref. [9], the proton gap still influences the next pairs, especially (94,142), according to the utilized theoretical model.

The action integral is minimized within the whole space of deformation. The deformation energy and the inertia tensor are calculated in the four-dimensional space of deformation with the components B_{ij} ($i, j = \chi_H, \chi_L, R_3, R$). The first two variables, χ_H and χ_L, are the semiaxis ratios of the heavy (H) and light (L) fragment, respectively. These quantities are free to vary between the initial parent (^{236}Pu) and the final fragment (^{144}Nd and ^{92}Se) values. This work chose different exponential laws of variation of the form

$$\chi_H = \chi_H^{\rm final} + \left(\chi_{\rm parent} - \chi_H^{\rm final}\right)\exp\left[-\left(\frac{R - R_k}{R - R_f}\right)^2\right] \tag{14}$$

for the heavy fragment, where R_k is a free parameter (it decides the distance whence χ_H starts to vary), and

$$\chi_L = \chi_L^{\rm final} + \left(\chi_{L0} - \chi_L^{\rm final}\right)\exp\left[-\left(\frac{R - R_k}{R - R_f}\right)^2\right] \tag{15}$$

for the light fragment, where χ_{L0} is a free variable between $\chi(^{236}\text{Pu})$ and the final value $\chi_L(^{92}\text{Se})$.

The procedure for obtaining the tensor components implies the free variable differentials; so the law of variation for χ_H and χ_L permits us to calculate $d\chi_i$ as a function of the distance between centers R. One has to stress here that complying with these laws does not restrict in any way the freedom of variation for χ_H and χ_L. It is only an analytical means to cover all the points in the deformation space between their initial and final values. The R_3-dependent components are obtained from the volume conservation and the variation of the heavy and light spheroidal parts and the neck region volumes. The coupling components are expressed as

$$B_{ij}(q) = \pi\sigma_m \int_{z_m}^{z_M} T_{ij}(z;q)dz, \tag{16}$$

with

$$T_{ij}(z;q) = \rho_s^2(z;q)\left[X_i(z)X_j(z) + \frac{1}{8}\rho_s^2(z;q)\frac{\partial X_i}{\partial z}\frac{\partial X_j}{\partial z}\right], \tag{17}$$

where σ_m is the mass density and ρ_s is the ρ value on the nuclear surface as a function of all free variables q. The couplings between different degrees of freedom are included in the T_{ij} term of the above equation. The quantities $X_i^{(k)}$ express the change of an infinitesimally thin slice of volume (∂V) with the change of the free parameter, like R_3 in the following Eq. (17). The idea of Wheeler was to divide the nuclear shape in thin circular disks that change their radius and position in conjunction with the deformation change, i.e., with the variation of every degree of freedom independently. The term T_{ij} is in fact the infinitesimal change of the shape-volume of the thin slice with respect to the volume conservation and irrotational motion. Every change in the i deformation variable induces a change in the j deformation variable. The total number of permutations i-j between the degrees of freedom describing the deformation defines the components of the inertia tensor. The influence of the fragment deformations on the inertia tensor, and hence on the dynamics, is included in the couplings that involve χ_H and χ_L. The neck component depends on

$$X_{R_3}^{(k)}(z) = \frac{1}{\rho_s^{(k)2}(z;q)}\frac{\partial V^{(k)}}{\partial R_3}, \tag{18}$$

where $V^{(k)}$ is the volume of $k = H$ (heavy), L (light), and (neck)-region successively. As the volumes vary with the distance between centers R, the χ_{R_3} components can be calculated numerically. A correction term is also added to each

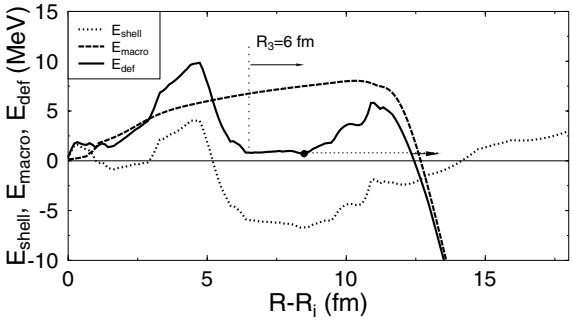

FIG. 3. The deformation energy $E_{\rm def}$, shell corrections $E_{\rm shell}$, and liquid drop energy $E_{\rm macro}$ along the fission path projected on the R direction.

B_{ij} to account for the center of mass displacement [12], and the whole tensor is contracted along the R direction. Finally one calculates the action integral S within the multidimensional space of deformation as

$$S(L^{(\rm fis)}) = \frac{2}{\hbar}\int_{L^{(\rm fis)}} [2E_{\rm def}(R, q(R))B(R, q(R))]^{1/2} dR, \quad (19)$$

where

$$B(R, q(R)) = \sum_{i,j} B_{ij}\frac{dq_i}{dR}\frac{dq_j}{dR} \quad (20)$$

and $L_{\rm fis}$ is the multitude of all possible fission paths. In the expression of the action integral $B(R, q(R))$ stands for the contracted tensor along R, and q takes the place of all other free coordinates. The fact that one considers the deformation parameters as depending on R does not restrict their freedom of variation. Their change with R according to Eqs. (13) and (14) is just a means to populate every point of the multidimensional grid of the deformation space. When the minimization of the action integral is performed, the system is free to move between every two existing points in the integrand value mesh of the action S.

IV. RESULTS AND DISCUSSION

The dynamic barrier obtained by the minimization of the action integral within the multidimensional space of deformation [13] is presented in Fig. 3. The large deep gap displayed by the shell corrections $E_{\rm shell}$ (pointed line) lowers the barrier (solid line) in the range of $R = 6$ to 10 fm between centers. The gap influence appears at $R_3 = 6$ fm and is very strong, so that the nuclear configuration preserves this neck value from thereon up to the exit point from the barrier ($R = 13.7$ fm). The deformed minimum is marked with a full circle at 8.2 fm with a deformation energy $E_{\rm def} = 0.9$ MeV against the ^{236}Pu ground state.

As a result of the multidimensional minimization of the action integral, the penetrability ln (P) has been calculated using the WKB formula, along the distance between centers. The variation of the tensor of inertia along the fission path projected on the ($R - R_i$) plane (where R_i is the initial distance between centers) in units of m_0 (proton mass) is displayed in the upper part of Fig. 4. The sudden increase of the neck radius R_3 is

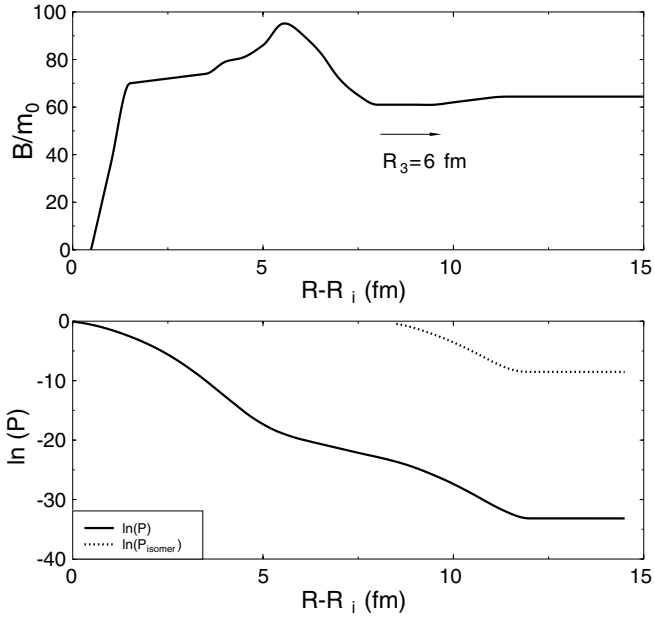

FIG. 4. The penetrabilities along the dynamical path for the fission channel ^{144}Nd + ^{92}Se. The solid line represents the penetrability from the ground state, whereas the dotted line is the penetrability from the deformed isomer minimum in Fig. 3.

observed on $B(q)$ as a bump around $R - R_i = 6$ fm. From the inertial point of view, the system opposes the change toward a large neck. After $R - R_i \approx 8$ fm, the tensor does not change very much, approaching the reduced mass value. In the lower part of Fig. 4, the variation of the logarithmic penetrability ln (P) is traced along the distance between centers, for the mass and charge asymmetry channel ^{144}Nd + ^{92}Se. The solid line represents the penetrability variation from the ground state of ^{236}Pu, whereas the dotted line shows the variation starting from the deformed minima isomeric state, marked in Fig. 3. The difference is about 20 orders of magnitude, but to reach the isomeric state the system must achieve around 1 MeV excitation energy against the ground state.

V. CONCLUSION

The neck potential is derived from the potential theory starting with an oscillator type force between nucleons. The neck potential smoothly links the spheroidally deformed oscillators of the two fission fragments. The spin-orbit term is added and the transition level scheme for protons and neutrons is obtained for binary necked configuration. The calculations for the fission of ^{236}Pu show that at a value of the neck radius $R_3 = 6$ fm a gap at the proton Fermi level develops and its effect is a minimum in the total shell correction energy that could accommodate a shape isomer state along the ^{92}Se + ^{144}Nd fission channel. The gap appears only when the neck parameter varies around $R_3 = 6$ fm and the corresponding minimum in the proton shell correction is deep enough to produce a pocket in the total deformation energy. The penetrability is obtained by minimization of the action integral along this particular fission channel. Its value

calculated from the ground state up to the exit point of the barrier is about 20 orders of magnitude smaller than the one obtained when starting from the deformed isomeric minimum configuration.

ACKNOWLEDGMENTS

This work was supported by the Romanian Ministry of Education and Research, the CEEX Program, and the IDEI Program, CNCSIS, Bucharest.

[1] M. Bosterli, E. O. Fiset, J. R. Nix, and J. L. Norton, Phys. Rev. C **5**, 1050 (1972).
[2] U. Brosa and S. Grossmann, Z. Phys. A **310**, 177 (1983).
[3] F. A. Ivanyuk, H. Hofmann, V. V. Pashkevich, and S. Yamaji, Phys. Rev. C **55**, 1730 (1997).
[4] G. Royer and B. Remaud, J. Phys. G **10**, 1541 (1984).
[5] Raj K. Gupta, M. Balasubramaniam, R. Kumar, D. Singh, C. Beck, and W. Greiner, Phys. Rev. C **71**, 014601 (2005).
[6] J. Maruhn and W. Greiner, Z. Phys. **251**, 431 (1972).
[7] R. A. Gherghescu, Phys. Rev. C **67**, 014309 (2003).
[8] V. Strutinsky, Nucl. Phys. **A95**, 420 (1967).
[9] L. Dematte, C. Wagemans, R. Barthelemy, P. D. D'Hondt, and A. Deruytter, Nucl. Phys. **A617**, 331 (1997).
[10] J. Okolowicz, J. M. Irvine, and J. Nemeth, J. Phys. G **9**, 1385 (1983).
[11] V. Metag and G. Sletten, Nucl. Phys. **A282**, 77 (1977).
[12] R. A. Gherghescu and D. N. Poenaru, Phys. Rev. C **72**, 027602 (2005).
[13] R. A. Gherghescu, J. Skalski, Z. Patyk, and A. Sobiczewski, Nucl. Phys. **A651**, 237 (1999).